EurJIC
European Journal of Inorganic Chemistry

Chemistry Europe
European Chemical Societies Publishing

Accepted Article

Title: Unusually Large Singlet Oxygen (1O2) Production by Very Weakly Emissive Pyrene-Functionalized Iridium(III) Complex: Interplay between Excited 3ILCT/3IL and 3MLCT States

Authors: Sourav Kanti Seth and Pradipta Purkayastha

To be cited as: *Eur. J. Inorg. Chem.* 10.1002/ejic.202000442

Link to VoR: https://doi.org/10.1002/ejic.202000442

WILEY-VCH

10.1002/ejic.202000442

WILEY-VCH

Unusually Large Singlet Oxygen ($^1O_2$) Production by Very Weakly Emissive Pyrene-Functionalized Iridium(III) Complex: Interplay between Excited ^{3}ILCT/^{3}IL and ^{3}MLCT States

Sourav Kanti Seth, and Pradipta Purkayastha*

Dedication ((optional))

S. K. Seth, Prof. P. Purkayastha
Department of Chemical Sciences
Indian Institute of Science Education and Research (IISER) Kolkata
Mohanpur 741246, WB, India
E-mail: ppurkayastha@iiserkol.ac.in
Homepage: https://sites.google.com/site/pradiptp/

Supporting information for this article is given via a link at the end of the document.

Abstract: The photophysical properties of a few Ir(III) and Rh(III) complexes have been attempted to be correlated (**1-4**) with their $^1O_2$ generation efficiencies. A very weakly emissive pyrene-functionalized Ir(III) complex (**1**) produces $^1O_2$ more efficiently than the other more emissive Ir(III) complexes. All of them have excited triplet state lifetimes (τ_T) in the microsecond regime. However, the pyrene-functionalized Ir(III) complex possesses the largest τ_T and has reasonable HOMO (highest occupied molecular orbital) energy (< –5.51 eV) which is desired for efficient $^1O_2$ production. **1-4** emit mostly from the ^{3}MLCT state. The lowest triplet emissive state of **3** and **4** is the ^{3}MLCT state while it is the ^{3}ILCT/^{3}IL state for **1** which is mostly non-emissive. However, the large excited state lifetime and the small energy gap between the ^{3}ILCT/^{3}IL states and the ground electronic state for complex **1** facilitates efficient energy transfer to molecular $^3O_2$ producing $^1O_2$.

Introduction

In the past few decades, luminescent transition metal complexes have been explored, studied and applied extensively in various fields of biology, organic electronic materials, photo-redox catalysis, etc. Among all these the Ru(II),[1,2] Os(II)[3,4] and Pt(II)[5,6] complexes were most extensively studied because of their rich photophysical properties, whereas the Ir(III), Rh(III), Re(I) complexes were less explored. The Ir(III) complexes are of special interests because of their superior and tunable photophysical as well as photochemical properties and vivid uses in several applications, such as, organic light-emitting diodes (OLED),[7-9] light-emitting electrochemical cells (LEEC),[10,11] dye-sensitized solar cells (DSSC),[12,13] photo-redox catalysts,[14] bioimaging,[15-17] photodynamic therapy (PDT), etc.[18-20] It is known that the excited electronic states of a metal complex depend on the metals and ligands present in it. For example, keeping the strong field polyimine ligands common, the nature of emissive excited electronic states of the complexes are dictated by the presence of different transition metals.[21] For 4d elements like Ru(II), Rh(III), etc., the MC (metal centered d-d transitions) states are low lying (i.e., possessing small octahedral field strength, Δ) and thermally accessible to the ^{3}MLCT/^{3}ILCT/^{3}IL states (metal-to-ligand charge transfer (MLCT) or intraligand charge transfer (ILCT) or intraligand (IL) triplet states) rendering energy dissipation in a non-radiative way. On the other hand, the 5d element Ir(III) makes the MC states to lie at higher energy (large octahedral field strength, Δ) which is thermally less accessible to the emissive ^{3}MLCT states. Consequently, the emission occurs radiatively from ^{3}MLCT resulting into a significantly large emission quantum yield. Inclusion of either of the aforementioned heavy metals in organic chromophores would render the intersystem crossing (ISC) with almost 100% efficiency (i.e., $\phi_{ISC} \approx 1$). Not only the heavy atoms contribute in dictating the nature of the triplet states (^{3}MLCT/^{3}ILCT/^{3}IL) but ligands also play an important role. Usually Ir(III) complexes, having phenanthroline or bipyridine derivatives as ancillary ligands, are predominantly ^{3}MLCT populated in their excited state and show a lifetime around ~1μs with reasonable emission quantum yield.[22,23] However, there are a few chromophoric groups (polynuclear aromatic hydrocarbons, such as, pyrene, anthracene, etc.), which are attached to the ancillary ligands, are reported to have ^{3}ILCT/^{3}IL populated excited states with longer excited species lifetime (few μs) and very less emission quantum yield. Some recent reports have shown that inclusion of one pyrene moiety to Ir(III) or Ru(II) complexes raises the excited state lifetime significantly from a few hundred ns to several μs.[24-28] This has led us to incorporate one pyrene moiety to the coordination complexes used in the present study. Coordination complexes of Ru(II)bipyridyl with phen-imidazolyl-pyrene (pyip) ligand are reported to have very small emission quantum yield because of the presence of low lying ^{3}ILCT/^{3}IL states that lead to non-radiative decay.[29-31] However, anthracene functionalized Ir(III) complexes are reported to get photooxidized and unstable to light due to the reactive anthracene moiety.[32] On the contrary, the complex becomes very stable on replacing the anthracece unit with pyrene.

In PDT, singlet oxygen ($^1O_2$), which is a reactive oxygen species (ROS), is used to treat tumor cells. Because of the large value of the spin-orbit coupling constant of Ir (ζ_{Ir} = 3909 cm^{-1}),[21] Ir(III) complexes undergo significant ISC in their excited electronic states, thus incorporating more triplet character and long excited state lifetimes (~μs range) making them more favorable to transfer charge or energy to other suitable systems.

Molecular oxygen is a well-known quencher of the excited triplet states of phosphors in its stable triplet state ($^3O_2$) where charge transfer converts to various types of ROS such as, $^1O_2$, superoxide ions ($O_2^{\cdot-}$), peroxide ions (O_2^{2-}), hydroxyl radical ($OH^{\cdot}$), under different conditions. Singlet oxygen ($^1O_2$) is generated by energy transfer from the excited electronic states of the complexes to $^3O_2$.[18,33,34] Among the ROS mentioned above, $^1O_2$ is known to be the most reactive and hence useful in PDT.

Normally, $^1O_2$ has two energy states: the higher energy, $^1\Sigma^+_g$ and the lower energy, $^1\Delta_g$.[33] Several photosensitizers are reported to produce $^1O_2$. The highest occupied molecular orbital (HOMO) energy levels (preferably lower than –5.51 eV), emission wavelength (emissive energy gap, 1.63 – 2.21 eV) and the emission quantum yield of the photosensitizer together is the key factor for $^1O_2$ generation.[18] Hence, we synthesized the ligand **L1** (see Supporting Information) and a new pyrene-functionalized Ir(III) complex (**1**) and measured its $^1O_2$ generation efficiency to compare with similar compounds (**2**-**4**) (Figure 1).[35,36] To examine the generation of $^1O_2$ we have used suitable standards.[37-39] Calculation of the different energy levels showed that the energy gap between the ^{3}ILCT and the ground state is much smaller in case of **1** compared to that for **2**-**4** where the energies of the ^{3}MLCT and ^{3}ILCT are close to each other.[29,30] The ^{3}ILCT energy of **1** matches well with the energy required to convert $^3O_2$ to $^1O_2$. Hence, proficient energy transfer is predictable from **1** to $^3O_2$ for its efficient conversion to $^1O_2$. Based on the results, we have proposed the principal requirements that a sensitizer must possess to become an efficient $^1O_2$ generator.

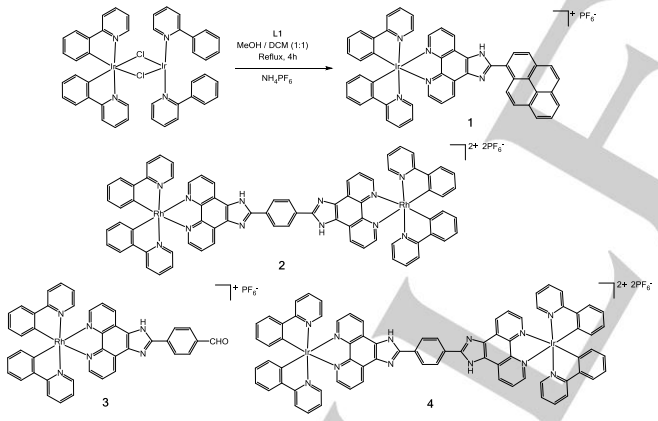

Figure 1. Synthetic route for **1** and structures of **2**, **3** and **4**.

Results and Discussion

Absorption spectroscopy results

Absorption spectrum of **1** in acetonitrile shows similar kind of bands to those of **2**-**4** which were already reported by us (Figure 2).[35,36] Bands peaking at 280 nm and 375 nm are attributed to the spin-allowed singlet π-π* ligand-to-ligand charge transfer (^{1}LLCT) or intra-ligand charge transfer (^{1}ILCT) and spin-allowed singlet metal-to-ligand charge transfer (^{1}MLCT) electronic transitions, respectively. A very weak shoulder in the range 440-470 nm is probably due to spin-forbidden ^{3}MLCT transition. All the complexes are found to be highly photostable since they do not show any notable change in the absorption spectra when exposed to 375 nm laser light (50 mW) continuously for 30 minutes (Figure 3).

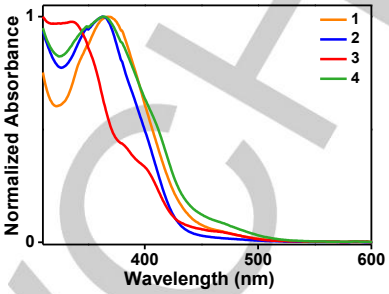

Figure 2. The absorption spectra of 20 μM of the complexes **1**-**4** in acetonitrile.

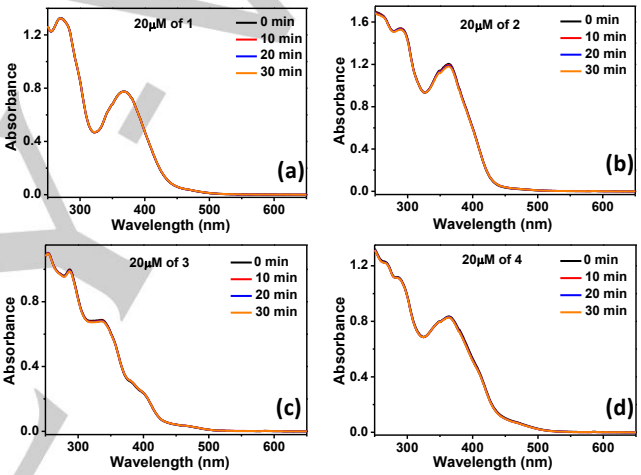

Figure 3. Photostability of the complexes **1**-**4** in acetonitrile.

Since all the complexes have quite long excited state lifetimes (in μs) (shown later), they are anticipated to transfer either their charge (referred as Type I process) or excited triplet state energy (referred as Type II process) to molecular oxygen ($^3O_2$) to produce various ROS including $^1O_2$. The $^1O_2$ generation can be detected in two ways: (i) direct method - that allows the detection of the emission of $^1O_2$ at 1268 nm: O_2 ($^1\Delta_g$) → O_2 ($^3\Sigma^-_g$) + hν (1268 nm) and (ii) indirect method - where photophysical changes of the molecular probes which react with the ROS are monitored, using specific small molecules, such as, 1,3-diphenylisobenzofuran (DPBF),[40-43] 3,3'-diaminobenzidine (DAB),[40,44] 1,5-dihydroxynaphthalene (DHN), etc.[24,45-47] In the present work DPBF, which is specific for $^1O_2$ detection, has been used. DPBF is a highly light sensitive probe and easily gets photolysed even to weak daylight in presence or absence of $^1O_2$ in many solvents.[42] While this is a drawback of using DPBF to monitor ROS, but if performed in dark the problems can be minimized. We have taken special care while doing these experiments since this compound has other advantages. DPBF absorbs in 300-450 nm wavelength range peaking at around 410-415 nm with a double hump at 310-325 nm. Any light within this wavelength range eventually causes photolysis of DPBF.

Since the complexes absorb at around 370 nm, we used a 375 nm laser that falls within the aforementioned range of wavelengths and photolysed DPBF. The rate of photolysis is faster in acetonitrile and relatively slow in acetonitrile-TBS mixture and even slower in DMSO. Photolysis or oxidation of DPBF produces 1,2-dibenzoylbenzene (DBB) which neither absorbs nor emits in the visible region.

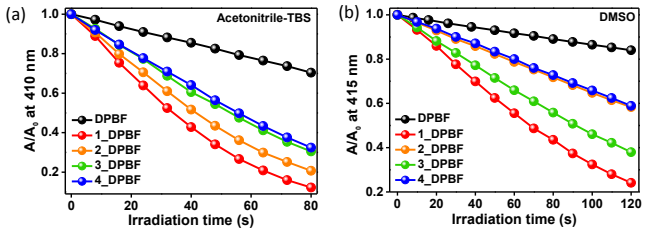

Figure 4. Degradation of DPBF compared from the changes in absorbance in air-equilibrated (a) 3:2 acetonitrile-TBS mixture and (b) DMSO monitored at 410 nm and 415 nm, respectively with irradiation (375 nm) time.

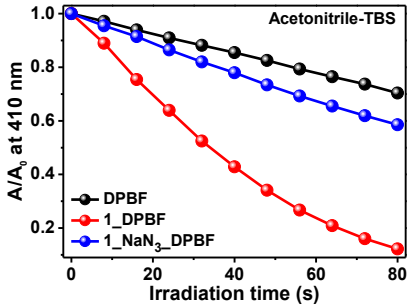

Figure 5. Relative change in absorbance of DPBF in presence of **1** with respect to irradiation time and NaN_3 (100 mM) in air-equilibrated 3:2 acetonitrile-TBS mixed solvent.

The efficiencies of the different complexes under study (**1**-**4**) for $^1O_2$ generation vary with solvent characteristics which is observable from the relative changes in absorbance at 410 nm (in acetonitrile-TBS) (Figure 4a) or 415 nm (in DMSO) (Figure 4b) with irradiation time. In 3:2 acetonitrile-TBS mixture, the efficiency of $^1O_2$ generation of the complexes follows the order: **1**>**2**>**3**>**4**; whereas, in DMSO this becomes: **1**>**3**>**2**≈**4**. Generation of $^1O_2$ is inhibited by few singlet oxygen scavengers, such as, sodium azide (NaN_3),[48,49] histidine,[40] etc. We used NaN_3 to confirm the generation of $^1O_2$ further. N_3^- ion reacts with $^1O_2$ to form $N_3^{\bullet}$, thus rendering $^1O_2$ unavailable to react with DPBF (Figure 5).[48,49] The extent of $^1O_2$ quenching by NaN_3 is maximum for **1** in comparison to the others (**2**-**4**). This suggests that ROS produced by **1** is mainly $^1O_2$ whereas **2**-**4** produce $^1O_2$ along with other ROS which were not tested any further.

The well-known $^1O_2$ sensitizers, methylene blue (MB) and meso-tetraphenylporphyrin (TPP), were applied to compare the efficiency of $^1O_2$ production by **1**-**4**. Since the rate of self-photolysis of DPBF is solvent dependent, benzene was the solvent of choice in our experiment since the quantum yield for $^1O_2$ generation with TPP as standard in benzene is reported in literature. In this case, the relative change in absorbance of DPBF with irradiation time was calculated from that at 315 nm since TPP absorbs strongly at 418 nm. This is possible since the slope of the A/A_0 vs. time plots considering both 315 nm and 410 nm, which was previously obtained from DPBF degradation in DMSO, is nearly the same (Figure S1). $^1O_2$ generation quantum yield (Table 1) is found to be maximum for **1** (ϕ_Δ = 0.73) with respect to TPP (ϕ_Δ = 0.62) on excitation at 355 nm, whereas it is found to be less for **2**-**4** (ϕ_Δ = 0.45 – 0.59). $^1O_2$ generation (in terms of % degradation of DPBF) by **1**-**4** was also compared with TPP and MB with light irradiation in the entire visible range. It follows similar trend as the $^1O_2$ quantum yield with **1**. The $^1O_2$ quantum yield of MB and TPP had been reported previously in dichloromethane and benzene, respectively. The rate of photolysis of DPBF under visible light is so fast in the aforementioned two solvents that degradation in presence of $^1O_2$ could hardly be measured. However, the photolysis rate of DPBF is much slower in DMSO, and hence DMSO was chosen herein as the solvent for all the sensitizers. Since the molar extinction coefficients of TPP and MB are much larger in visible region than those of **1**-**4**, they absorb the visible light more than **1**-**4** producing more $^1O_2$ (Figure S2).

Table 1. Photophysical parameters for $^1O_2$ generation by complexes **1**-**4**

Species	λ_{abs}[a] (nm)	λ_{em}[a] (nm)	ϕ^{em}[b]	τ_T[b] (μs)	k_r[c] (10^5 s^{-1})	k_{nr}[c] (10^5 s^{-1})	ϕ_Δ[d]	ϕ_{rel}[e]
1	368	574	0.0011 (0.0033)	1.15 (5.08)	0.010	8.69	0.73	0.77
2	363	574	0.0013 (0.0024)	2.52 (2.17)	0.005	3.97	0.56	0.48
3	338	581	0.0174 (0.076)	1.20	0.145	8.19	0.59	0.59
4	365	582	0.0378 (0.076)	0.91	0.415	10.57	0.45	0.44
TPP	-	-	-	-	-	-	0.62	>0.97
MB	-	-	-	-	-	-	-	0.92

[a] λ_{abs} and λ_{em} are obtained in acetonitrile. [b] ϕ_{em} are the emission quantum yields and τ_T are the lifetimes of the triplet excited species obtained from nanosecond flash photolysis and measured in 3:2 acetonitrile/aqueous solution and in neat acetonitrile (values in parenthesis). [c] k_r is the radiative rate constant and k_{nr} is the non-radiative rate constant, which are calculated from ϕ_{em} and τ_T using the equations $k_r = \phi_{em} / \tau_T$ and $\tau_T = 1/(k_r + k_{nr})$ in 3:2 acetonitrile/aqueous solution. [d] ϕ_Δ is $^1O_2$ generation quantum yield with respect to TPP (ϕ_Δ= 0.62) in benzene. [e] ϕ_{rel} is the relative efficiency of $^1O_2$ generation in DMSO in terms of % DPBF degradation under white light irradiation.

Steady state emission spectroscopy results

Since all the complexes have triplet excited state population, their emissions are greatly affected by the presence of molecular oxygen ($^3O_2$) which is a well-known quencher of excited triplet state. **3** and **4** show bright emission on excitation at 375 nm peaking at around 580 nm due to the predominant ^{3}MLCT population. **2** emits very weakly with maxima at 475 nm and 570 nm due to the emission from the admixture of ^{1}LC/^{1}MLCT and ^{3}LC/^{3}MLCT states. A previous low temperature study showed that the ^{3}MLCT state is the lowest emissive triplet state in **4** and both the ^{3}MLCT and the ^{3}LC emissive states are closely spaced in **2**.[50] Similar to **2**, **1** shows a weak emission band with a maximum at 573 nm that could be originating from the ^{3}LC/^{3}MLCT states. Literature reports on Ru(II) complexes with ligand **L1** mention two distinct triplet states, ^{3}MLCT and ^{3}IL/^{3}ILCT, among which the first one is indicated to be emissive and higher energy state, while the latter as the non-emissive and lowest triplet state.[29,51] Likewise, **1** shows very small emission quantum yield (ϕ_{em} = 0.003) consistent with the reported data for the Ru(II)-**L1** complexes (Table 2). The emission quantum yields for **3** and **4** are quite large (ϕ_{em} ≈ 0.23) and that for **2** is very small (ϕ_{em} < 0.002) evidently because of the presence of the thermally accessible non-emissive ^{3}MC state (Table 2).

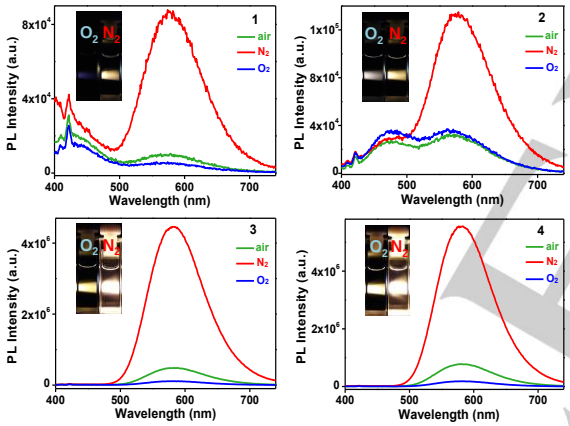

Figure 6. Emission spectra of **1-4** in air-equilibrated, degassed, oxygenated acetonitrile solution excited at 375 nm.

Since triplet state emission for all the complexes appears in the same spectral range with similar emission maximum (570-580 nm), their emission is expected to occur from similar energy states, which are the ^{3}MLCT/^{3}MLLCT (metal to ligand charge transfer, $d\pi_{Ir}\rightarrow\pi^*_{phen}$ or metal-ligand to ligand charge transfer, $(d\pi_{Ir}+\pi_{ppy})\rightarrow\pi^*_{phen}$) states. Moreover, consistent with the literature reports, **1** is expected to have ^{3}ILCT/^{3}IL state as its lowest triplet state which is non-emissive and a higher energy emissive ^{3}MLCT state. However, emission from the singlet excited states of **1** and **2** does not seem to be much altered in presence of O_2 or N_2. Emission from all the complexes shows significant dependence on the environment (inert or aerobic). Complexes **1-4** show 3 to 7-fold enhancements in emission quantum yield on going from air-equilibrated to degassed solvents. Similarly, complexes **1**, **3** and **4** show 2 to 4-fold decrease in emission intensity at 580 nm on oxygenation of the air-equilibrated solvents, whereas emission intensity remains almost unchanged for **2**. These situations have been depicted in Figure 6.

Table 2. Emission quantum yield (ϕ_{em}) of **1-4** in air-equilibrated and degassed solvents.

Complex	Condition	Dichloromethane	Acetonitrile	Acetonitrile-TBS
1	Air	0.0008	0.0012	0.0007
	N_2	0.0019	0.0033	0.0011
2	Air	0.0006	0.0008	0.0007
	N_2	0.0011	0.0024	0.0013
3	Air	0.044	0.0116	0.0098
	N_2	0.229	0.076	0.0174
4	Air	0.042	0.011	0.0125
	N_2	0.235	0.076	0.0378

The lifetime of the excited states studied by time correlated single photon counting (TCSPC)

1-4 also show significant environment dependent (inert or aerobic) emission lifetimes in the TCSPC study (Figure 7 and Table 3). Being more interested to the longer lifetime components that govern the emission from the triplet excited states, the decay measurements were made in the forward mode with longer time to amplitude conversion (TAC) range (1 μs). The long lifetime components appear due to the presence of the ^{3}MLCT/^{3}ILCT states and are very much affected by the presence of O_2 and N_2 in the solution. However, **1**, **3** and **4** show similar emission decays and lifetimes (244 – 286 ns) in presence of N_2 and O_2 and are expected to have similar emissive state ^{3}MLCT. Among these compounds, **2** is very low emissive. The average lifetimes are calculated using the equation, $\langle\tau\rangle = \Sigma\alpha_i\tau_i/\Sigma\alpha_i$, where the τ_i values denote lifetimes of individual components and α_i are the contributions of the respective components.

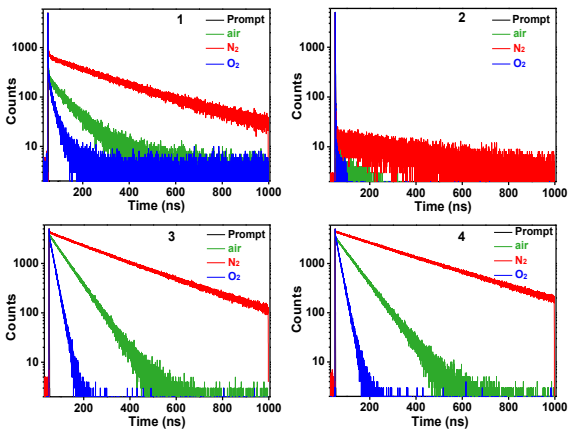

Figure 7. Emission decay (TCSPC) profiles of **1-4** in air-equilibrated, degassed, oxygenated acetonitrile solution excited at 375 nm.

Table 3. Emission lifetimes (TCSPC) of **1-4** in air-equilibrated, degassed, oxygenated acetonitrile solutions excited at 375 nm. The χ^2 values indicate the goodness of the fits and the data are within ±5% error limit.

Complex	Condition	τ_1 (ns) (a_1 %)	τ_2 (ns) (a_2 %)	τ_3 (ns) (a_3 %)	χ^2
1	Air	83.1 (82.25)	0.22 (11.65)	3.3 (6.10)	1.21
	N_2	254.6 (98.0)	0.61 (2.0)	-	1.26
	O_2	25.3 (53.25)	0.25 (30.76)	3.2 (15.99)	1.24
2	Air	0.78 (70.17)	0.31 (29.83)	-	1.27
	N_2	396.4 (53.61)	0.16 (22.84)	0.78 (23.56)	1.17
	O_2	3.6 (2.79)	0.60 (97.21)	-	1.22
3	Air	64.3 (100)	-	-	1.18
	N_2	244.7 (100)	-	-	1.11
	O_2	17.6 (98.71)	0.39 (1.29)	-	1.18
4	Air	69.2 (100)	-	-	1.30
	N_2	286.7 (100)	-	-	1.06
	O_2	17.6 (98.72)	0.76 (1.28)	-	1.19

It is pertinent to mention here that two different experimental set-ups have been used to obtain the excited state lifetimes of the complexes: (a) time correlated single photon counting (TCSPC) involves detection of emissive photons arriving at different time delays and is an emission based technique with the detection range of few hundreds of picoseconds to few hundreds of nanoseconds; (b) nanosecond transient absorption (ns TA) obtained from flash photolysis set-up that involves the principle of absorption spectroscopy with few hundreds of nanoseconds to few hundreds of microseconds (µs) timescale. Since Ir and Rh complexes µs lifetimes for the excited triplet state, these are well obtained from ns TA, whereas, the spontaneous radiative lifetimes are obtained from the TCSPC technique. At this point, it is worth mentioning that the longer triplet species do not necessarily decay in a radiative way to the ground state, rather non-radiative decay rates are more facilitated. Hence, the total (radiative + non-radiative) triplet state lifetimes are obtained from the positive band of the TA spectra and only the radiative spontaneous lifetimes are obtained from TCSPC.

Computational study

Studies using density functional theory (DFT) and time-dependent DFT (TDDFT) on [**1**–PF_6]$^+$ provide a clear picture of the molecular orbital (MO) energy levels and the major electronic transitions involved during excitation. The electron density in HOMO is centered mostly on pyrene and a lesser extent over the imidazole part, whereas that in the LUMO is localized on the phenanthroline moiety, making HOMO→LUMO transition at 451.99 nm (Table 4) to be ^{1}ILCT ($\pi_{pyrene}\rightarrow\pi^*_{phen}$) type. Other higher energy transitions also have ^{1}ILCT/^{1}IL ($\pi_{pyrene}\rightarrow(\pi^*_{phen} + \pi^*_{pyrene})$) character showing H→(L+1) and H→(L+2) electronic transitions and strong oscillator strengths (403.84 nm, f = 0.6480 and 379.25 nm, f = 0.3050, respectively).

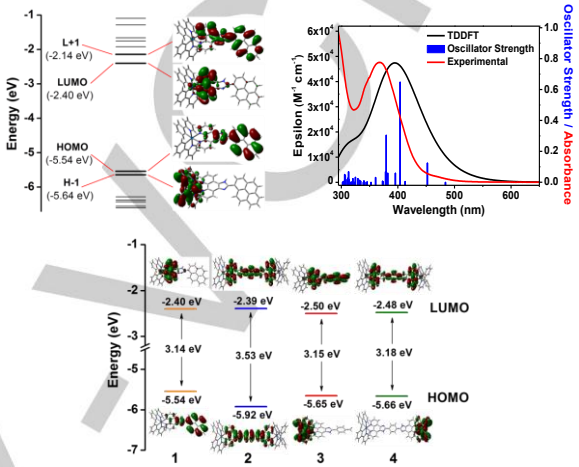

Figure 8. (Top) frontier MOs (molecular orbitals), corresponding energy levels and comparison of absorption spectra obtained theoretically and experimentally in acetonitrile for complex **1**; (bottom) HOMO-LUMO energy-levels diagram for complex **1-4** obtained via DFT calculations.

Table 4. Major electronic transitions involved during excitation of complex [**1**-PF_6]$^+$. H and L stand for HOMO and LUMO.

Complex	Experimental λ_{abs}(nm) (εx10^{-3} M^{-1}cm^{-1})	Calculated λ_{abs}(nm) (f = oscillator strength)	Major transitions (Contribution)	Assignment
[**1**-PF_6]$^+$	458 (2.4)	451.99 (f=0.1246)	H→L (97%)	ILCT $\pi_{pyrene}\rightarrow\pi^*_{phen}$
	402 (22.4)	403.84 (f=0.6480)	H→(L+1) (92%)	ILCT/IL $\pi_{pyrene}\rightarrow(\pi^*_{phen} + \pi^*_{pyrene})$
	369 (38.8)	379.25 (f=0.3050)	H→(L+2) (56%) (H–1)→(L+4) (13%) (H4)→L (13.9%)	ILCT, $\pi_{pyrene}\rightarrow\pi^*_{phen}$, IL $\pi_{ppy(Ir)}\rightarrow\pi^*_{ppy}$, MLCT/MLLCT $(d\pi_{Ir} + \pi_{ppy})\rightarrow\pi^*_{phen}$

However, for **2-4** ($-PF_6^-$), only HOMO and LUMO electron densities are studied by DFT in acetonitrile using the PCM methodology (Figure 8). Both HOMO and LUMO of **2** are localized on the whole ancillary ligand (central bridging ligand), suggesting electronic transition with ^{1}ILCT/^{1}IL character. It is very interesting to note at this point that HOMO and LUMO of **2** in gaseous state are centred on the Rh/ppy ligand and the ancillary ligand, respectively, thus allowing the ^{1}MLCT/^{1}MLLCT

type transitions.[50] Both **3** and **4** show ^{1}MLCT/^{1}MLLCT/^{1}LLCT type transitions in both gaseous and solution (acetonitrile) state since HOMO and LUMO are localized on the Ir/ppy ligand and the ancillary ligand, respectively. HOMO and LUMO energy levels (in eV), as obtained from the DFT study for **1-4**, possess similar values except a little extra stabilization of the HOMO for **2** that could have resulted because of the slightly higher electronegativity of Rh atom than Ir.

Cyclic voltammetric analysis

Cyclic voltammetry (CV) helps to find the frontier molecular orbitals (FMO) of the complexes experimentally. The HOMO and LUMO were obtained from the CV data and the absorption spectra of the respective complexes (Figure 9). HOMO were calculated from the onset oxidation potential of the complexes using the equation, E_{HOMO} (eV) = –(4.4 + E_{ox}^{onset}).[52] HOMO-LUMO energy gaps were obtained from the onset peaks of the absorption spectra: ΔE (eV) = 1240 (nm) / λ_{onset} (nm). LUMO were calculated using the above-mentioned values of E_{HOMO} and ΔE as, E_{LUMO} (eV) = E_{HOMO} + ΔE. The order of the HOMO of the complexes follow quite well with those obtained from the computational studies (Table 5). The HOMO level of **1** (i.e., -5.44 eV) is found to be least stabilized among all the other complexes due to the dominance of the IL or ILCT over MLCT. This drives the electron density more towards the metal center compared to that in **3** or **4**, where electronic transition is more of MLCT character. The HOMO of **2** (i.e., –5.63 eV) is most stabilized because of slightly higher electronegativity of the Rh center making it more reluctant to get oxidized. On the other hand, LUMO of the complexes deviate slightly from the order obtained from the computational studies. Energy of the emissive triplet state (E_T) for **1-4** is obtained using E_T (eV) = (E_{HOMO} + 1240 (nm) / λ_{em} (nm)).

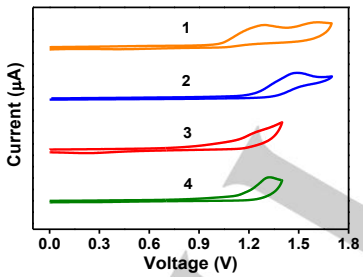

Figure 9. Cyclic voltammograms of **1-4** in acetonitrile with a scan rate of 100 mV s^{-1}.

Table 5. Energy levels of frontier orbitals obtained experimentally for **1-4** in acetonitrile.

Complex	Condition (eV)	τ_1 (ns) (a_1 %)	τ_2 (ns) (a_2 %)
1	– 5.44	– 2.62	– 3.28
2	– 5.63	– 2.74	– 3.47
3	– 5.49	– 2.65	– 3.36
4	– 5.54	– 2.76	– 3.41

Flash photolysis results and analysis

Nanosecond flash photolysis study provided a deeper insight into the lifetimes of the excited state transient species upon excitation with 355 nm laser light. Flash photolysis spectra of **1** show similar kind of absorption in acetonitrile and acetonitrile-TBS mixture (Figure 10). A band with negative absorption at around 370 nm corresponds to the ground state bleaching of **1**. A positive strong absorption band starting from just above 400 nm and tailing at over 700 nm corresponds to the triplet charge transfer excited species, mainly, ^{3}IL/^{3}ILCT and, to a lesser extent, ^{3}MLCT. Lifetime of the excited species of complex **1** absorbing at 560 nm varies slightly from solvent to solvent. In acetonitrile, triplet species lifetime at 560 nm is 5.08 μs, while it is 1.15 μs in acetonitrile-TBS solution. Similar spectra were obtained for complex **2** (Figure S3), showing a negative band for ground state bleach at around 360 nm and a positive broad band between 400 to 700 nm. The positive broad band may be attributed to the ^{3}ILCT/^{3}MLCT species having lifetimes 2.17 and 2.52 μs in acetonitrile and acetonitrile-TBS solutions, respectively. However, for complexes **3** and **4**, the lifetimes of the excited triplet species (predominantly from ^{3}MLCT) are taken from our previous study, i.e., 1.15 μs and 0.91 μs in aceotonitrile-aqueous solution since their photophysical properties are analogous to that in the acetonitrile-TBS solution.[36] It is difficult to obtain signal for the absorption by the excited species in acetonitrile because of their strong stimulated emission.

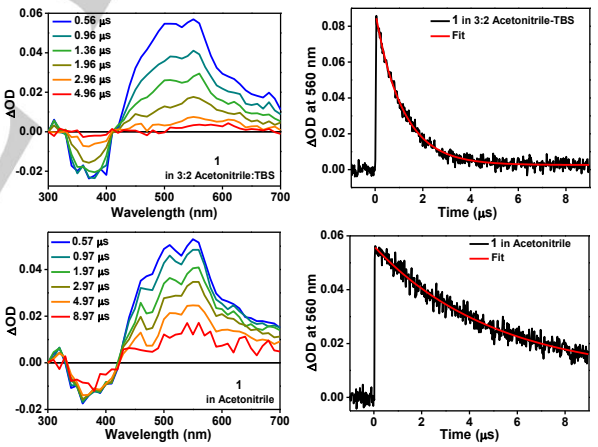

Figure 10. Nanosecond flash photolysis spectra of **1** and their corresponding decay-fits in 3:2 acetonitrile-TBS (top) and acetonitrile (bottom).

The proposed energy levels

Because of the presence of the Ir(III) center, **1**, **3** and **4** have the ^{3}MC states at much higher energy than the emissive ^{3}MLCT/^{3}ILCT states. Nevertheless, **1** has low emission quantum yield due to the presence of low lying non-emissive ^{3}ILCT/^{3}IL states. Less emission quantum yield and emission wavelength, which is similar to that of **2-4,** also suggest presence of higher energy and less populated ^{3}MLCT state. However, results from DFT calculations and relatively large emission quantum yield of **3** and **4** suggest the presence of low lying emissive ^{3}MLCT states which could be closely spaced with the ^{3}ILCT state. On

the other hand, because of the presence of the Rh(III) center in **2**, the ^{3}MC state lies closer to the emissive ^{3}MLCT/^{3}ILCT states and is thermally accessible rendering excited triplet state to decay in non-radiative way. This discussion has been summarized in Figure 11. Thus, the mechanism proposes that the 254 ns lifetime component of **1** is the emissive lifetime that occurs from the higher lying ^{3}MLCT states even in the presence of the low lying ^{3}ILCT states. For **1**, the ^{3}MLCT states get affected by molecular oxygen that sensitizes the conversion of $^3O_2$ to $^1O_2$. Additionally, the ^{3}ILCT states would also sensitize the transformation. Since for **1**, ^{3}ILCT is much more populated than ^{3}MLCT, the major emphasis was on the ^{3}ILCT states that eventually produce more $^1O_2$. Hence, the ^{3}MLCT states of **1** would also produce $^1O_2$.

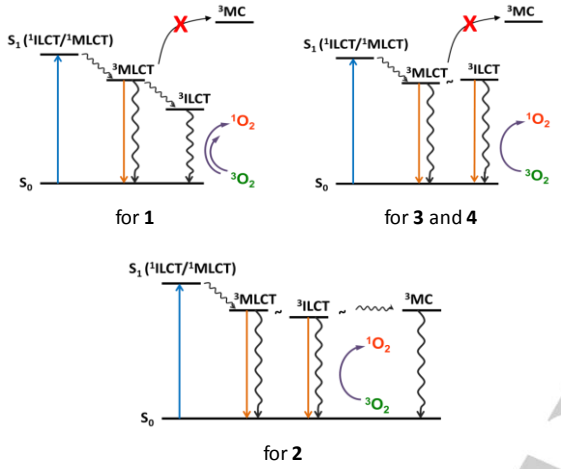

Figure 11. Schematic of the energy levels for complexes **1-4**.

Conclusion

We have synthesized a new pyrene-functionalized Ir(III) complex (**1**), characterized photophysically and compared with **2-4**. Their $^1O_2$ generation efficiencies are also measured and compared. Interestingly, in spite of its very low emission quantum yield, **1** produces more $^1O_2$ than **2-4** among which **3** and **4** are much more emissive and **2** has emission analogous to **1**. Even though, they primarily have ^{3}MLCT state as the emissive state, only **1** has mainly ^{3}ILCT/^{3}IL as the lowest triplet excited state which is non-emissive and much lower in energy (>574 nm). This is in contrary to the existing literature where it has been predicted that for efficient generation of $^1O_2$ the photosensitizer must have large emission quantum yield.[18] Based on the results obtained, we have proposed a new set of essential requirements for a sensitizer to be an efficient $^1O_2$ generator. Necessarily, the molecule must possess a reasonable HOMO energy level (preferably lower than –5.51 eV). The triplet excited state lifetime must be long (in µs range) with small energy gap preferably close to 762 nm which is the gap between ground state $^3O_2$ and the second excited state of $^1O_2$ existing between the lowest triplet excited state and the ground state. The emission quantum yield (large or small) is not a necessary requirement in this process.

Experimental Section

Materials

$IrCl_3$. xH_2O, 2-phenylpyridine (ppy), 1,10-phenanthroline, 1-pyrenecarboxaldehyde, pyrrole, bezaldehyde, methylene blue (MB), terephthalaldehyde, 1,3-diphenylisobenzofuran (DPBF), sodium azide (NaN_3), tris buffered saline (TBS) tablets, quinine hemisulfate were of >99% purity and purchased from Sigma-Aldrich. The procured chemicals were used as received. Solvents used for the syntheses were of analytical grade and those used for spectroscopic measurements were of spectroscopy grade. HPLC water was used as and when required.

The precursor $[Ir(ppy)_2Cl]_2$ was prepared following the literature procedure.[53] **2**, **3** and **4** were synthesized according to the method reported by us previously.[35,36] Ligand **L1** was synthesized following literature procedure and used without further purification (see Supporting Information) .[31] TPP was synthesized following a modified literature procedure and characterized with ^{1}H NMR (Figure S4) and ESI-MS (Figure S5).

Synthesis of 1

L1 (50.4 mg, 0.12 mmol) and $[Ir(ppy)_2Cl]_2$ (53.6 mg, 0.05 mmol) were taken in 1:1 dichloromethane/methanol mixture (30 ml) in a round-bottom flask and refluxed for 4 h. The mixture was allowed to settle down to the room temperature and excess of KPF6 was added to the solution to precipitate out the yellow product. The solvent was evaporated in reduced pressure using a rotary evaporator and the crude product was purified by column chromatography using 1-7% methanol in dichloromethane as eluent to obtain an orange yellow product. The product was characterized using ^{1}H NMR spectroscopy (Figure S6) and ESI-MS (Figure S7).

Acknowledgements

The financial support from the Science and Engineering Research Board, Government of India through the project CRG/2018/000555 is gratefully acknowledged. Facility of flash photolysis obtained from Saha Institute of Nuclear Physics is thanked by the authors. SKS acknowledges the Council of Scientific and Industrial Research for his fellowship. The authors are thankful to Dr. Parna Gupta of IISER Kolkata for useful discussions and helping in synthesizing the ligands and the complexes.

Keywords: Singlet oxygen • emissive states • pyrene-functionalized Ir(III) complex • ^{3}MLCT states • ^{3}ILCT/^{3}IL states

[1] F. E. Poynton, S. A. Bright, S. Blasco, D. C. Williams, J. M. Kelly, T. Gunnlaugsson, *Chem. Soc. Rev.* **2017**, *46*, 7706.
[2] M. R. Gill, J. A. Thomas, *Chem. Soc. Rev.* **2012**, *41*, 3179.
[3] J. P. Sauvage, J. P. Collin, J. C. Chambron, S. Guillerez, C. Coudret, V. Balzani, F. Barigelletti, L. De Cola, L. Flamigni, *Chem. Rev.* **1994**, *94*, 993.
[4] C. Creutz, M. Chou, T. L. Netzel, M. Okumura, N. Sutin, *J. Am. Chem. Soc.* **1980**, *102*, 1309.
[5] K. M.-C. Wong, W.-S. Tang, B. W.-K. Chu, N. Zhu, V. W.-W. Yam, *Organometallics* **2004**, *23*, 3459.

[6] C. M. Che, C. C. Kwok, S. W. Lai, A. F. Rausch, W. J. Finkenzeller, N. Zhu, H. Yersin, *Chem. Eur. J.* **2010**, *16*, 233.
[7] C. H. Yang, Y. M. Cheng, Y. Chi, C. J. Hsu, F. C. Fang, K. T. Wong, P. T. Chou, C. H. Chang, M. H. Tsai, C. C. Wu, *Angew. Chem. Int. Ed.* **2007**, *46*, 2418.
[8] C.-F. Chang, Y.-M. Cheng, Y. Chi, Y.-C. Chiu, C.-C. Lin, G.-H. Lee, P.-T. Chou, C.-C. Chen, C.-H. Chang, C.-C. Wu, *Angew. Chem. Int. Ed.* **2008**, *47*, 4542.
[9] M. S. Lowry, S.; Bernhard, *Chem. Eur. J.* **2006**, *12*, 7970.
[10] T. Hu, L. He, L. Duan, Y. Qiu, *J. Mater. Chem.* **2012**, *22*, 4206.
[11] H. J. Bolink, L. Cappelli, E. Coronado, M. Gratzel, E. Orti, R. D. Costa, P. M. Viruela, M. K. Nazeeruddin, *J. Am. Chem. Soc.* **2006**, *128*, 14786.
[12] E. Baranoff, J.-H. Yum, I. Jung, R. Vulcano, M. Gratzel, M. K. Nazeeruddin, *Chem. Asian J.* **2010**, *5*, 496.
[13] D. D. Wang, Y. Wu, H. Dong, Z. X. Qin, D. Zhao, Y. Yu, G. Zhou, B. Jiao, Z. X. Wu, M. Gao, G. Wang, *Org. Electron.* **2013**, *14*, 3297.
[14] C. Yang, F. Mehmood, T. L. Lam, S. L.-F. Chan, Y. Wu, C.-S. Yeung, X. Guan, K. Li, C. Y.-S. Chung, C.-Y. Zhou, T. Zou, C.-M. Che, *Chem. Sci.* **2016**, *7*, 3123.
[15] J. Liu, Y. Liu, Q. Liu, C. Li, L. Sun, F. Li, *J. Am. Chem. Soc.* **2011**, *133*, 15276.
[16] K. K.-W. Lo, K. Y. Zhang, *RSC Adv.* **2012**, *2*, 12069.
[17] L. Xiong, Q. Zhao, H. Chen, Y. Wu, Z. Dong, Z. Zhou, F. Li, *Inorg. Chem.* **2010**, *49*, 6402.
[18] J. S. Nam, M. G. Kang, J. Kang, S. K. Park, S. J. C. Lee, H. T. Kim, J. K. Seo, O. H. Kwon, M. H. Lim, H. W. Rhee, T. H. Kwon, *J. Am. Chem. Soc.* **2016**, *138*, 10968.
[19] C.-W. Lai, Y.-H. Wang, C.-H. Lai, M.-J. Yang, C.-Y. Chen, P.-T. Chou, C.-S. Chan, Y. Chi, Y.-C. Chen, J.-K. Hsiao, *Small* **2008**, *4*, 218.
[20] L. K. McKenzie, I. V. Sazanovich, E. Baggaley, M. Bonneau, V. Guerchais, J. A. G. Williams, J. A. Weinstein, H. E. Bryant, *Chem. Eur. J.* **2017**, *23*, 234.
[21] L. Flamigni, A. Barbieri, C. Sabatini, B. Ventura, F. Barigelletti, *Top. Curr. Chem.* **2007**, *281*, 143.
[22] A. J. Howarth, D. L. Davies, F. Lelj, M. O. Wolf, B. O. Patrick, *Inorg. Chem.* **2014**, *53*, 11882.
[23] S. Guo, K.-K. Chen, R. Dong, Z.-M. Zhang, J. Zhao, T.-B. Lu, *ACS Catal.* **2018**, *8*, 8659.
[24] A. J. Hallett, N. White, W. Wu, X. Cui, P. N. Horton, S. J. Coles, J. Zhao, S. J. A. Pope, *Chem. Commun.* **2012**, *48*, 10838.
[25] Y. Lu, J. Wang, N. McGoldrick, X. Cui, J. Zhao, C. Caverly, B. Twamley, G. M. Ó Maille, B. Irwin, R. Conway-Kenny, S. M. Draper, *Angew. Chem. Int. Ed.* **2016**, *55*, 14688.
[26] J. Peng, X. Jiang, X. Guo, D. Zhao, Y. Ma, *Chem. Commun.* **2014**, *50*, 7828.
[27] Y. Lu, R. Conway-Kenny, J. Wang, X. Cui, J. Zhao, S. M. Draper, *Dalton Trans.* **2018**, *47*, 8585.
[28] X. Jiang, J. Peng, J. Wang, X. Guo, D. Zhao, Y. Ma, *ACS Appl. Mater. Interfaces* **2016**, *8*, 3591.
[29] C. Reichardt, M. Pinto, M. Wachtler, M. Stephenson, S. Kupfer, T. Sainuddin, J. Guthmuller, S. A. McFarland, B. Dietzek, *J. Phys. Chem. A* **2015**, *119*, 3986.
[30] M. Stephenson, C. Reichardt, M. Pinto, M. Wachtler, T. Sainuddin, G. Shi, H. Yin, S. Monro, E. Sampson, B. Dietzek, S. A. McFarland, *J. Phys. Chem. A* **2014**, *118*, 10507.
[31] M. Mariappan, B. G. Maiya, *Eur. J. Inorg. Chem.* **2005**, *2005*, 2164.
[32] T.-B. Gao, Z.-Z. Qu, Z. Tang, D. K. Cao, Dalton Trans. 2017, 46, 15443.
[33] M. C. DeRosa, R. J. Crutchley, *Coord. Chem. Rev.* **2002**, *233−234*, 351.
[34] P. Zhang, C. K. C. Chiu, H. Huang, Y. P. Y. Lam, A. Habtemariam, T. Malcomson, M. J. Paterson, G. J. Clarkson, P. B. O'Connor, H. Chao, P. J. Sadler, *Angew. Chem. Int. Ed.* **2017**, *56*, 14898.
[35] S. K. Seth, S. Mandal, P. Purkayastha, P. Gupta, *Polyhedron* **2015**, *95*, 14.
[36] S. K. Seth, P. Gupta, P. Purkayastha, *New J. Chem.* **2017**, *41*, 6540.
[37] F. Wilkinson, W. P. Helman, A. B. Ross, *J. Phys. Chem. Ref. Data* **1993**, *22*, 113.
[38] R. W. Redmond, J. N. A. Gamlin, *Photochem. Photobiol.* **1999**, *70*, 391.
[39] P. I. Djurovich, D. Murphy, M. E. Thompson, B. Hernandez, R. Gao, P. L. Hunt, M. Selke, *Dalton Trans.* **2007**, 3763-3770.
[40] H. Kawasaki, S. Kumar, G. Li, C. Zeng, D. R. Kauffman, J. Yoshimoto, Y. Iwasaki, R. Jin, *Chem. Mater.* **2014**, *26*, 2777.
[41] P. Majumdar, X. Yuan, S. Li, B. Le Guennic, J. Ma, C. Zhang, D. Jacquemin, J. Zhao, *J. Mater. Chem. B* **2014**, *2*, 2838.
[42] X.-F. Zhang, X. Li, *J. Lumin.* **2011**, *131*, 2263.
[43] R. H. Young, D. Brewer, R. A. Keller, *J. Am. Chem. Soc.* **1973**, *95*, 375.
[44] G. A. Johnson, E. A. Ellis, H. Kim, N. Muthukrishnan, T.Snavely, J.-P. Pellois, *PLoS One* **2014**, *9*, e91220.
[45] D. Maggioni, M. Galli, L. D'Alfonso, D. Inverso, M. V. Dozzi, L. Sironi, M. Iannacone, M. Collini, P. Ferruti, E. Ranucci, G. A. D'Alfonso, *Inorg. Chem.* **2015**, *54*, 544.
[46] S. Takizawa, R. Aboshi, S. Murata, *Photochem. Photobiol. Sci.* **2011**, *10*, 895.
[47] J. Sun, J. Zhao, H. Guo, W. Wu, *Chem. Commun.* **2012**, *48*, 4169.
[48] J. R. Harbour, S. L. Issler, *J. Am. Chem. Soc.* **1982**, *104*, 903.
[49] M. Bancirova, *Luminescence* **2011**, *26*, 685.
[50] S. K. Seth, S. Mandal, K. Srikanth, P. Purkayastha, P. Gupta, *Eur. J. Inorg. Chem.* **2017**, *2017*, 873.
[51] C. Reichardt, K. R. A. Schneider, T. Sainuddin, M. Wachtler, S. A. McFarland, B. Dietzek, *J. Phys. Chem. A* **2017**, *121*, 5635.
[52] L. Leonat, G. Sbarcea, I. V. Branzoi, *UPB Sci. Bull. Ser. B Chem. Mater. Sci.* **2013**, *75*, 111.
[53] S. Sprouse, K. A. King, P. J. Spellane, R. J. Watts, *J. Am. Chem. Soc.* **1984**, *106*, 6647.

Entry for the Table of Contents

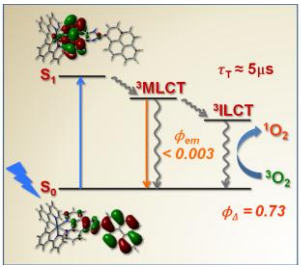

A very weakly emissive pyrene-functionalized Ir(III) complex possessing the longest triplet state lifetime and < -5.51 eV HOMO energy produces singlet oxygen more efficiently than the other more emissive Ir(III) complexes.